An Evaluation of the Accuracy of AIRS Radiances From Sea Surface Temperature Measurements

Denise Hagan
Jet Propulsion Laboratory,
California Institute of Technology

Introduction

Some aspects regarding the precision and accuracy of the AIRS spectrometer while viewing Earth during the initial six months of operation are described in this paper. Hagan and Minnett (2003) concluded that the required determination of accuracy of the instrument to an uncertainty of 0.5 K could be met in the initial validation exercises using surface marine observations. This paper demonstrates that the instrument is calibrated to within this accuracy in select window regions for scene temperatures ranging from 275 to 300 K.

The analyses presented here are based on two months of AIRS observations compared to buoy measurements co-located in space and time to within $\pm$50 km and two hours, respectively. The matchups are global and encompass a wide range of ocean temperatures and atmospheric conditions. Drifting buoys obtain measurements of sea surface temperature (SST) at depths approximately 10 to 15 cm below sea surface, with a calibration precision of 0.05^{o}C and an absolute accuracy of 0.1^{o}C (Sybrandy et al, 1995; G. Williams, personal communication).

The observations of this study are limited to night only conditions, to reduce uncertainties in the comparisons related to diurnal warming of the surface layer of the ocean in low wind speed regimes and to obviate effects of solar scattering. Oceanographic studies have shown that the gradient in surface layer density due to daytime solar heating is mixed away during the night by internal ocean mixing processes, in the absence of a freshwater barrier.

The basic procedure is to identify a set of cloud-free observations and compare the AIRS observed brightness temperatures with the corresponding buoy SST's. These comparisons are made at frequencies where the atmospheric transmission is maximized (i.e., in window regions where there are no discreet vapor phase absorptions, any residual absorption being due to diffuse (continuum) effects or to aerosols). A correction of the form

$$T\_surf(\upsilon)=BT\_{TOA}(\upsilon)+\alpha\sec(\theta) + \beta(\upsilon), \quad (1)$$

is applied to the observed TOA radiances to account for (i) the reduction of the sea surface radiance by atmospheric absorption, and (ii) the effect of non-unity in sea surface emission. The atmospheric correction term α, where θ is the instrument view angle, is determined from radiative transfer calculations using algorithms developed by Strow et al (2003) and Hannon et al (2003). The correction β was determined from the theoretical emissivity coefficients of Masuda et al. (1988). The dependence of emissivity on surface wind speed was not factored into the equation since the majority of observations

described here were obtained for nadir angles less than 40^o. The split window approach is used to determine the atmospheric absorption (McMillin, 1975). The basic premise is that the magnitude of the attenuation due to water vapor can be inferred from two spectral measurements that sub-divide the 800-1000 cm^{-1} window region (hence, split window). This technique has been applied to instruments that have broad spectral regions (~1 micron wide) centered at 11 and 12 microns (Prabhakara et al, 1974; McClain et al, 1985; Walton et al, 1988). The equation for this technique has the general form $SST = a_0 + a_1T_{11} + a_2(T_{11} - T_{12}) + a_4 (T_{11} - T_{12}) (\sec\theta - 1)$, where the regression coefficients are empirically derived. A similar technique was used to derive T_surf(υ), except α was determined by a simple binning method based on the difference between brightness temperatures in the window channels at 960 and 870 cm^{-1}.

Using this relationship, the adjustment of the top-of-atmosphere brightness (TOA) temperature to the surface is generally about +1 to +2 K in the shortwave region (2500-2700 cm^{-1}). In the longwave region (800-1200 cm^{-1}), the adjustments may be as large as +5 to +8 K for regions of high atmospheric moisture content (> 4 pr cm). The results of this report are focused on two window channels, 938 cm^{-1} and 2616 cm^{-1}, which are representative of the response of other window channels in these regions.

Analyses

The AIRS data and surface marine observations were co-located in time and space using resident software developed by the AIRS JPL team, known as matchup software. This software matches all relevant AIRS observations and surface truth parameters to within $\pm$ 50 km and $\pm$ two hours. Typically between 2500 and 3000 AIRS-buoy match-ups are obtained per day in clear and cloudy conditions; only 20 to 30 of these pass the clear sky test at night. This subset of the matchups was corrected to the surface using Equation 1 to obtain, essentially, AIRS SST. Over the period from September through October 2002, about 1400 cloud-free matchups were obtained at night.

The test for cloudiness is based on spatial homogeneity criteria. The matched data sets contain nine AIRS fields-of-view (eg., 3 x 3 pixel subsets). A set of nine pixels passes the cloud test if the maximum brightness difference between these fields of view is less than 1K for measurements at wavelengths of 900, 960 and 2616 cm^{-1}. Because cloud tends to lower the observed brightness temperature and may be undetected due to the large size of the AIRS footprint (15 km), the warmest pixel of the nine fields-of-view is selected for further study. However, it should be understood that this will produce a different result than if the central or an average of the nine pixels was selected. There are pros and cons in both cases. It was found that if the central pixel had been selected rather than the warmest pixel, the average difference between buoy SST and AIRS SST for the September-October data set (about 1400 observations) would be biased cooler by 0.1^oC.

The scatter diagrams in Figures 1-4 show uncorrected AIRS TOA brightness temperature observations compared with buoy SST, and the same set of AIRS observations corrected to the surface. The departures of buoy SST and AIRS brightness temperatures from perfect agreement tend to increase monotonically with increasing temperature (Figures 1,3). The AIRS data corrected to the surface show generally good agreement with the buoy observations (Figures 2,4), with the dispersion of the 938 cm^{-1}

measurements slightly greater than the 2616 cm^{-1} measurements. Statistical summaries of the difference statistics for these data sets are provided in the conclusions.

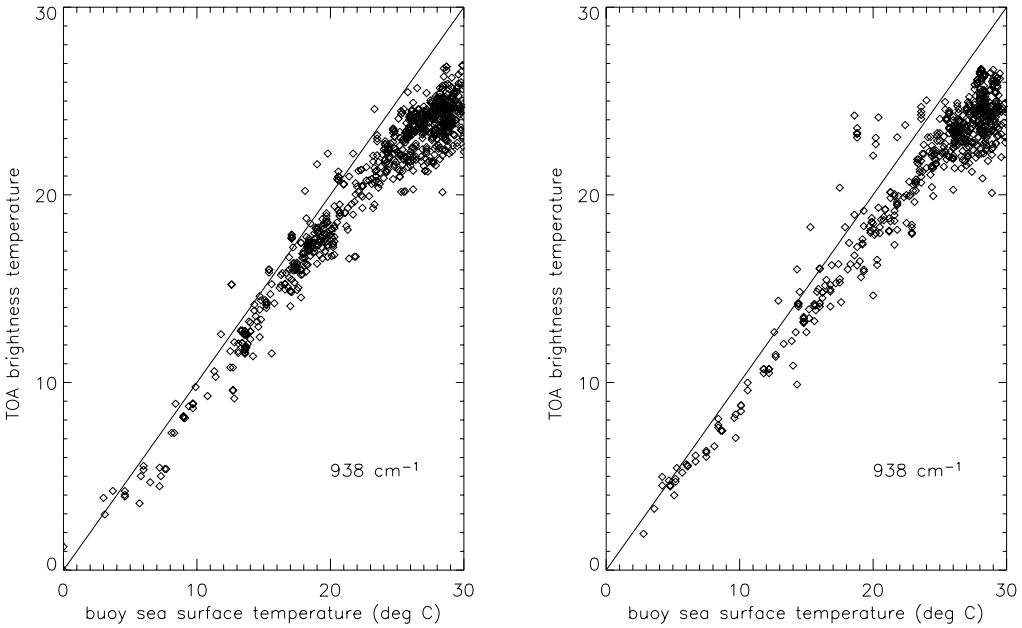

Figure 1. Scatter diagrams of buoy SST versus L1B TOA brightness temperatures at 938 cm^{-1} for (a) the month of September 2002, and (b) the month of October 2002.

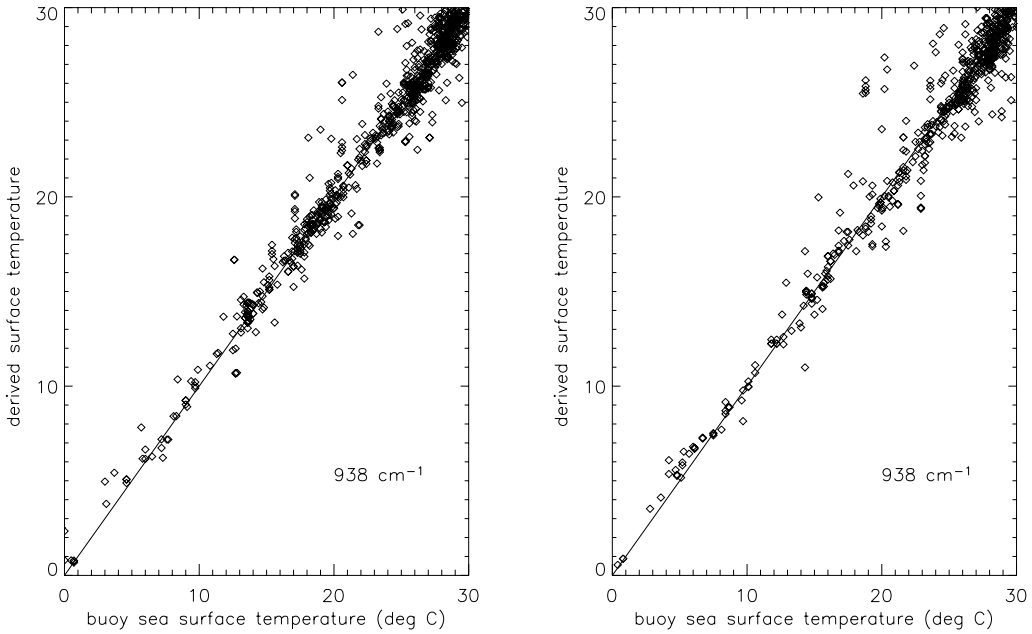

Figure 2. Scatter diagrams of buoy SST versus AIRS_SST_938 cm^{-1} (eg. L1B TOA brightness temperatures at 938 cm^{-1} that have been corrected to the surface) for (a) the month of September 2002, and (b) the month of October 2002.

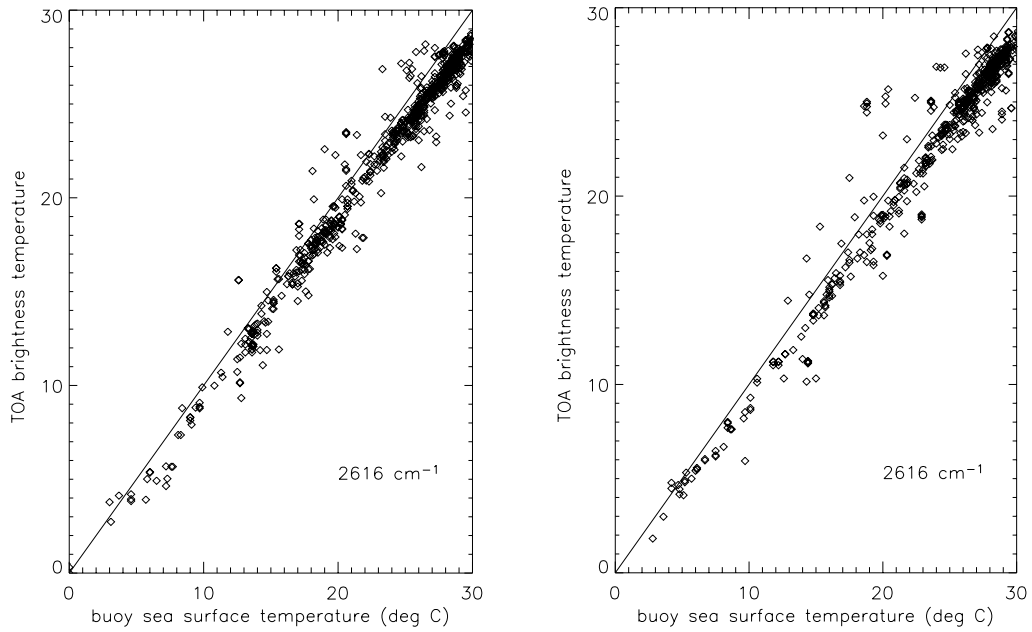

Figure 3. Scatter diagrams of buoy sea surface temperature versus L1B TOA brightness temperatures at 2616 cm^{-1} for (a) the month of September 2002, and (b) the month of October 2002. As in the case of the longwave region (Figure 1), the departure of AIRS data and buoy measurements from perfect agreement tends to increase with increasing temperature, except with less deviation.

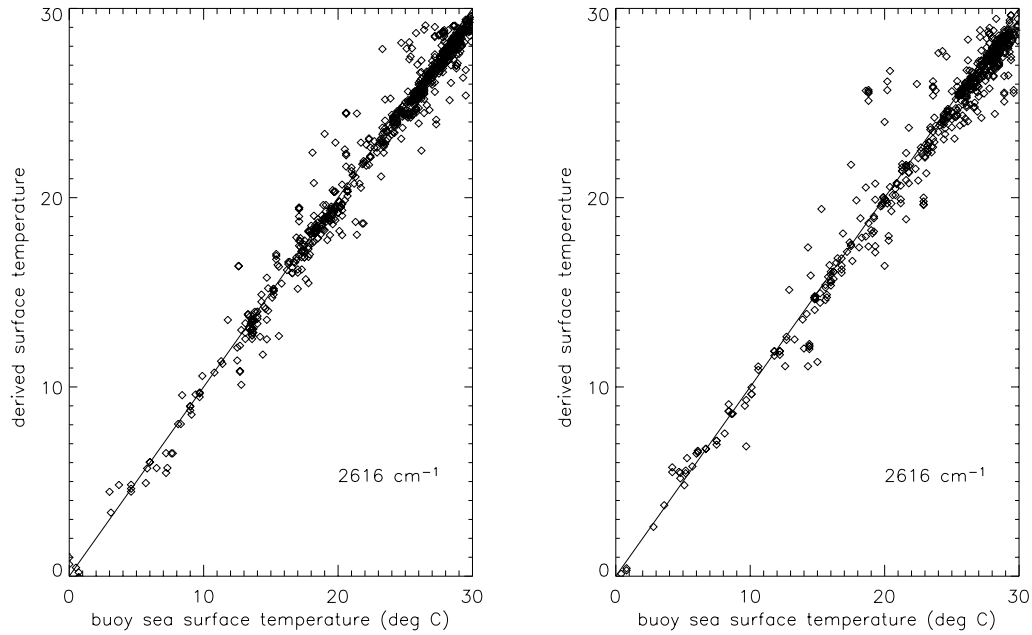

Figure 4. Scatter diagram of buoy SST versus AIRS_SST_2616 cm^{-1} (eg. L1B TOA brightness temperatures at 2616 cm^{-1} that have been corrected to the surface) for (a) the month of September 2002, and (b) the month of October 2002.

The scatter diagrams in Figure 5 show the magnitude of the corrections applied to the AIRS data (see Equation 1) as a function of split window brightness temperature differences. As the temperature differences between the split window measurements increase, the magnitude of the correction at 938 cm^{-1} increases. A much smaller dependence of the correction on split window temperature difference is observed at 2616 cm^{-1}. The surface emissivity corrections are larger than the corrections for atmospheric residual absorption at this wavelength.

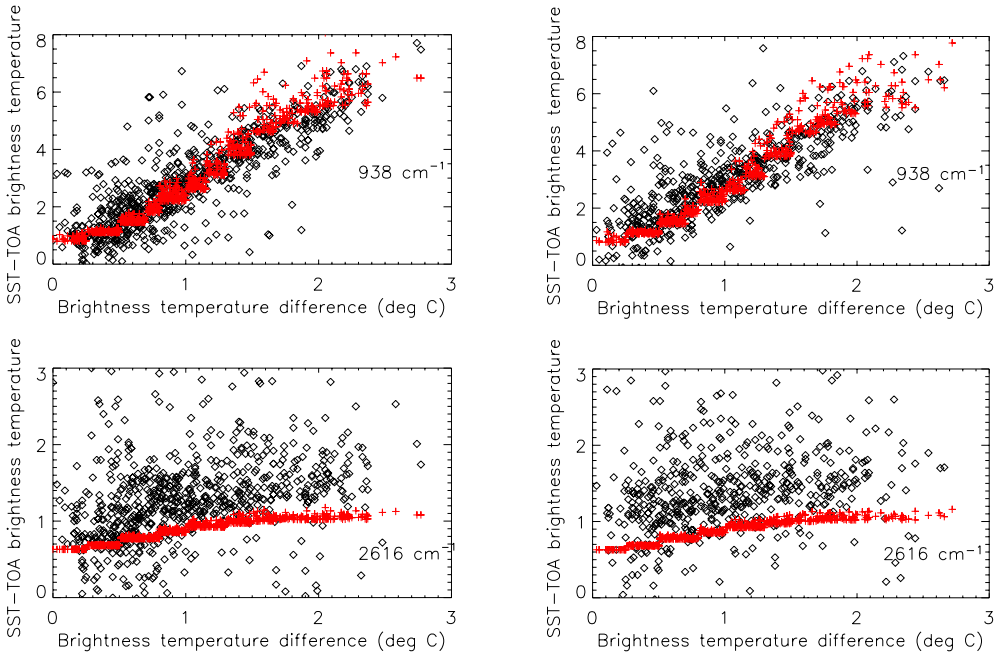

Figure 5. The relationship between split window brightness temperature differences and the magnitude of the corrections applied to AIRS TOA data at 938 cm^{-1} and 2616 cm^{-1} to obtain surface temperatures. The x-axes correspond to brightness temperature differences between two adjacent window regions (eg. split window). The y-axes correspond to SST – TOA brightness temperature at 938 cm^{-1} (upper panels) and 2616 cm^{-1} (lower panels). The black points represent differences when SST=buoy; the red points represent differences when SST=AIRS. Data are shown for months of September (left panels) and October (right panels).

The dispersions of the difference between AIRS SST and buoy SST as a function of latitude are shown in Figure 6. The data at 2616 cm^{-1} are biased cool relative to the buoy SST, with bias that is larger in the tropics. The data at 938 cm^{-1} show larger dispersion in the tropics, but the bias appears to be equally distributed as a function of latitude. Histograms for these data sets restricted to satellite view angles of $+30^0$ to -30^0 are shown in Figure 7. Both the shortwave and longwave channels are biased cool with respect to the buoy data.

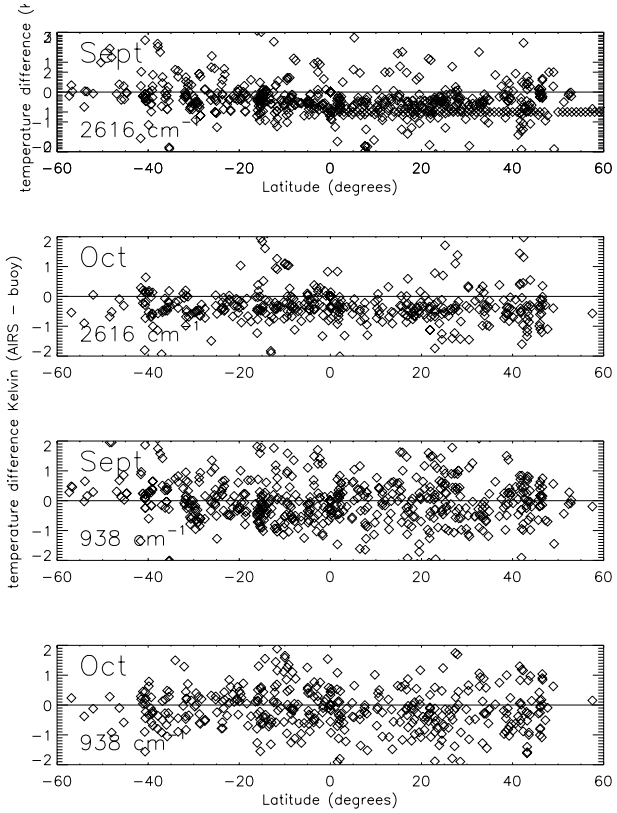

Figure 6. Upper two panels show temperature difference between AIRS_SST_2616 cm^{-1} and buoy SST versus latitude for months of September and October. Lower two panels show temperature distributions corresponding to AIRS_SST_938 cm^{-1}.

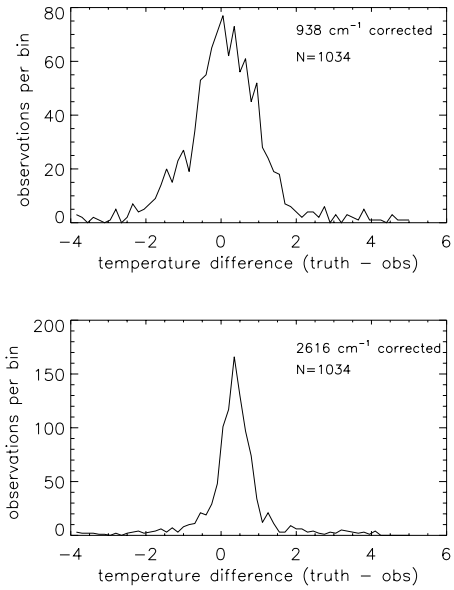

Figure 7. Histograms of the difference between buoy SSTs and AIRS derived surface temperatures, for global data restricted to satellite viewing angles between $+30^0$ and -30^0.

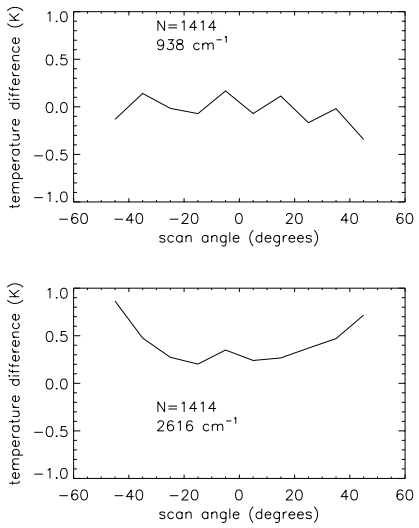

Figure 8. Temperature differences (SST_buoy – SST_AIRS) versus satellite view angle. The data are binned in intervals of 10 degrees.

The data of Figure 8 show a very coarse dependence of the difference between buoy SST and AIRS SST on satellite view angle. The SSTs derived from the 2616 cm^{-1} measurements show bias that increases as a function of view angle.

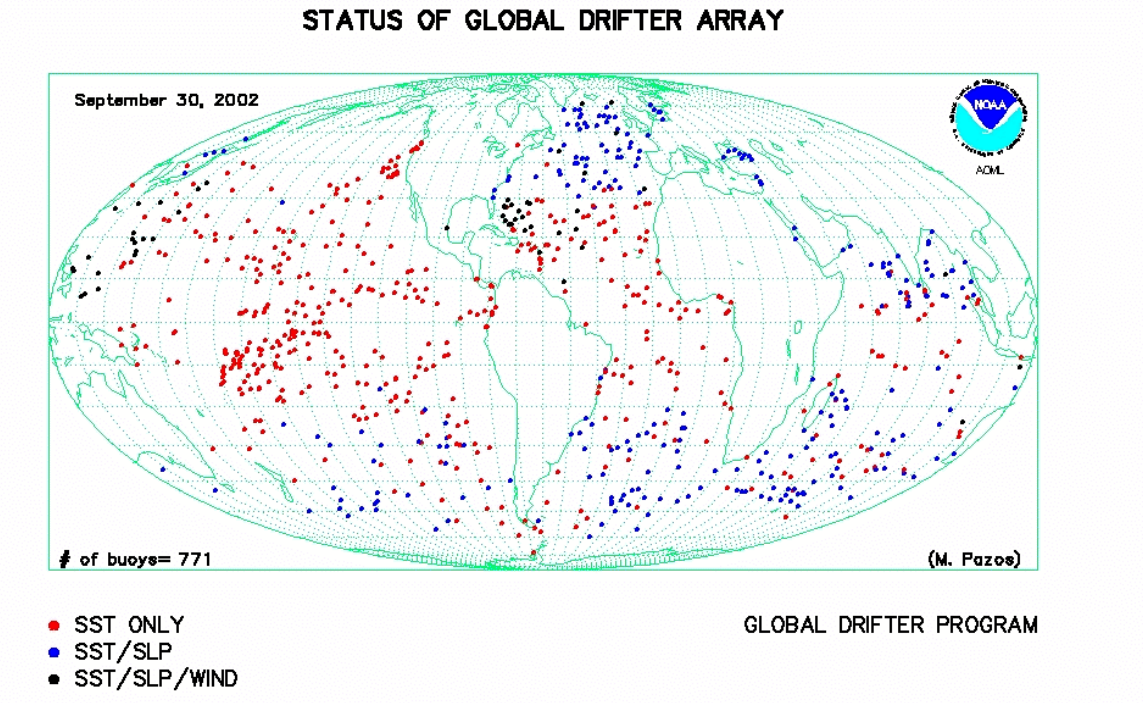

Figure 9. Global distribution of drifting buoys for the month of September 2002.

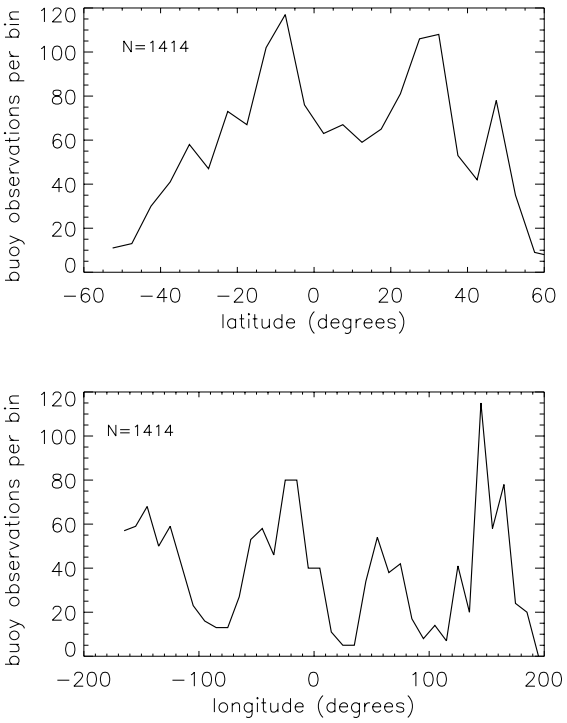

Figure 10. Distribution with latitude and longitude of matchup observations that passed cloud test for months of September and October 2002.

The geographic distribution of all data matchups is shown in Figure 9, and the distribution for night cloud-free matchups is shown in Figure 10. The peak at 12°S, 145°E is from a cluster of buoys located north of Australia. The entire range of ocean temperature in cloud-free conditions was sampled during the two months of observations, but the bulk of buoy–AIRS matchups were obtained in regions of SST greater than 25°C.

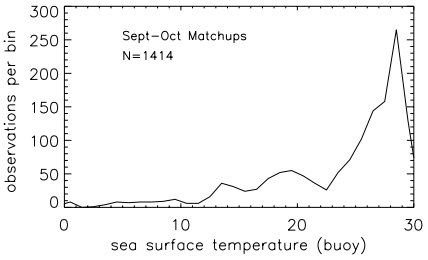

Figure 11. The distribution for buoy SST measurements used in this analysis, binned in 1°C intervals. The peak between 28-29°C represents about 20% of the observations.

Conclusions

Based on about 1400 match-up observations in relatively cloud-free, nighttime conditions, the following statements describe the response of the AIRS window channel at 938 cm^{-1}:

1) The first order behavior of the AIRS TOA radiance is consistent with what may be expected, as the TOA radiance tends to increase monotonically with increasing sea surface temperature. This behavior is expected under atmospheric conditions of normal adiabatic lapse rate and moisture content.

2) The TOA radiances were adjusted to be consistent with the sea surface radiance originating from the surface, using Equation 1. The corrected radiances (henceforth, AIRS_SST_$_{938\ cm^{-1}}$) are biased slightly warmer than the buoy SST for high atmospheric moisture content, and biased slightly cooler than the buoy SST for low atmospheric moisture content.

3) The global bias and standard deviation of the differences between AIRS_SST_$_{938\ cm^{-1}}$ and buoy_SST for two months of observations for all viewing angles is $-0.1 \pm 1.1^{o}C$. The dispersion of the data is affected by a small number of large outliers. If a normal distribution of data is assumed, the dispersion of 68% of the data centered about the mean is $\pm 0.6^{o}C$.

4) The dispersion of the data is approximately the same for all latitudes; there is no apparent latitude-dependent bias in the matchup comparisons.

5) The bias and standard deviation for the October data set ($-0.12 \pm 1.22\ ^{o}C$) are slightly larger than the bias and standard deviation for the September data set ($+0.01 \pm 0.90\ ^{o}C$), for comparisons limited to viewing angles between +30 and –30 degrees.

Based on about 1400 match-up observations in relatively cloud-free, nighttime conditions, the following statements describe the response of the AIRS window channel at 2616 cm^{-1}:

1) The first order behavior of the AIRS TOA radiance is consistent with what may be expected, as the TOA radiance tends to increase monotonically with increasing sea surface temperature.

2) The AIRS brightness temperatures and buoy SST show small but systematic differences when compared to model calculations; the data fall below expected values.

3) The global bias and standard deviation between AIRS_SST and buoy_SST for two months of observations for all viewing angles are $-0.3 \pm 1.1^{o}C$. The dispersion of the data

is affected by a small number of larger outliers. If a normal distribution of data is assumed, the dispersion of 68% of the data centered about the mean is $\pm$ 0.4^{o}C.

4) The bias and standard deviation for the October data set (-0.4 $\pm$ 1.1^{o}C) are slightly larger than the bias and standard deviation for the September data set (-0.23 $\pm$ 0.93^{o}C), for comparisons limited to viewing angles between +30 and –30 degrees.

5) The dispersion of the differences between buoy SST and AIRS data adjusted to the surface (AIRS_SST_2616 cm^{-1}) is lower in the tropics than in mid-latitudes, whereas the bias of the data distribution is larger in the tropics.

6) When the data sets are separated by geographic region, the bias in the mid-latitude data set (>30^{o}N, >30^{o}S) is negligible, whereas the bias for the tropics is –0.31^{o}C for the month of September and -0.48^{o}C for the month of October.

The mean global departures of AIRS observations from buoy SST measurements at night range from -0.3^{o}C to –0.5^{o}C for the shortwave region and from -0.1^{o}C to -0.2^{o}C for the longwave region, for data restricted to satellite viewing angles between +30 and -30 degrees. The comparisons are based on AIRS TOA measurements adjusted to the surface using the well known split window technique. The statistics are derived from a small population of numbers (~10^{3}). Although a wide range of ocean temperature conditions was sampled in this study, cold temperature regimes and high scan angles were sampled less frequently. Although the data sample is relatively small, no data selection has been carried out. The statistics are based on the average and standard deviation of all observations, including outliers. Median statistics or statistics that neglect the outliers will produce different numerical results. We have carried out validations in window regions and believe the instrument is calibrated to this accuracy over its entire spectral range, although this must remain an assumption until full retrievals are obtained in other spectral regions.

Validation studies by AIRS team members have shown different and sometimes larger discrepancies using other sources of truth, cloud detection and atmospheric modeling schemes. At the level of accuracy described here, small errors in the forward radiative transfer model, in cloud detection and the sea “truth” will influence the statistical results and can be difficult to separate. In a simulation study that examines these issues, Hagan and Minnett (2003) suggest that the ability to carry out statistical validation using surface marine observations can be accomplished with an accuracy of at least 0.5 K, taking into account the various sources of error. Their results also show that other sources of SST “truth” such as blended satellite and in situ data fields should produce similar global dispersions of data. For example, for September 6, 2002, buoy data matched with the NCEP SST-RTG product show bias differences in the tropics of just +0.02 $\pm$ 0.5^{o}C and in mid-latitudes -0.02 $\pm$ 0.8^{o}C (eg, the satellite data are almost exactly tied to the buoy data at the position of the buoys in the optimal interpolation schemes used for developing SST maps).

More accurate ‘skin surface’ validation comparisons should be achievable using MAERI ship-based observations. The MAERI is useful for addressing the evaporative

skin effect, a phenomenon that can result in differences of 0.1 to 0.3 K between bulk and radiometric measurements of SST. The buoy SSTs used in this study were not adjusted for this effect.

References

Hagan, D. and P. Minnett, "AIRS radiance validation over ocean from sea surface temperature measurements", *IEEE Transactions on Geosciences and Remote Sensing*, in press.

Hannon, S., L. Strow, S. Desouza-Machado, H. Motteler, D. Tobin."An Overview of the AIRS Radiative Transfer Model," in press, *IEEE Transactions Geosciences and Remote Sensing*, 2003.

Masuda, K., T. Takashima, and Y. Takayama, "Emissivity of pure and sea waters for the model sea surface in the infrared window region, *Rem. Sens. of Environ*., 24, 313-329, 1988.

McClain, E. P., W. Pichel, and C .Walton (1985), "Comparative performance of AVHRR-based multichannel sea surface temperatures". *J. Geophy. Research*., 90, 11587-11601.

McMillin, L. M., "Estimation of sea surface temperatures from two infrared window measurements with different absorption", *J. Geophy. Res*., 80, 5113-5117, 1975.

Pagano, T. S., H. H. Aumann, D.E. Hagan, and K. Overoye, "Prelaunch and in-flight radiometric calibration of the Atmospheric InfraRed Sounder (AIRS)", *IEEE Transactions on Geosciences and Remote Sensing*, in press.

Prabhakara, C., G. Dalu, and V. Kunde, "Estimation of sea surface temperature from remote sensing in the 11 to 13 micron window", ", *J. Geophy. Res*., 79, 5039-5044, 1974.

Strow, L., S. Hannon, M. Weiler, S. Gaiser and H. Aumann. "Spectral Calibration of the Atmospheric InfraRed Sounder**,**" in press, *IEEE Trans. Geosciences and Remote Sensing*, 2003

Sybrandy, A., C. Martin and P. Niiler, E. Charpentier, and D. Meldrum, WOCE surfce velocity programme barometer drifter construction manual, Data Buoy Co-operation Panel Report No. 4,WMO, Geneva, V. 1, Sept., 63 pp., 1995.

Walton, C., "Nonlinear multichannel algorithms for estimated sea surface temperatures with AVHRR satellite data. *J. Appl. Meteorol*., 27, 115-124.